

# Simultaneous Generation of Different Types of Ion Pairs upon Charge-Transfer Excitation of a Donor–Acceptor Complex Revealed by Ultrafast Transient Absorption Spectroscopy

Omar F. Mohammed<sup>†</sup> and Eric Vauthey\*

Department of Physical Chemistry, University of Geneva, 30 quai Ernest-Ansermet, CH-1211 Geneva 4, Switzerland

Received: February 2, 2008; Revised Manuscript Received: April 10, 2008

The excited-state dynamics of the methylperylene/tetracyanoethylene (MPe/TCNE) donor–acceptor complex has been investigated in various solvents using femtosecond transient absorption spectroscopy. The transient spectra reveal the formation of two types of ion pairs: The first (IP1), constituting the major fraction of the total ion-pair population, is characterized by a broad and red-shifted absorption spectrum compared to that of the free MPe cation and by a subpicosecond lifetime, whereas the second (IP2) has a spectrum closer to that of MPe cation and a lifetime of a few picoseconds. A substantial polarization anisotropy was observed with IP1 but not with IP2, indicating a relatively well-defined structure for the former. The reaction scheme that best accounts for the observed dynamics and its solvent dependence involves the simultaneous excitation of complexes that differ by their electronic coupling. The more coupled complexes have a high absorption coefficient and thus yield IP1, which undergoes ultrafast charge recombination, whereas the less coupled complexes have a lower probability to be excited and lead to the longer-lived IP2.

## Introduction

The charge-recombination (CR) dynamics of photogenerated ion pairs has been very intensively investigated over the past decade.<sup>1–6</sup> A detailed understanding of the factors that influence this energy-wasting process is of crucial importance for many practical applications. There are essentially two ways to produce ion pairs photochemically in a polar solvent: (1) bimolecular charge separation (CS) between a photoexcited molecule and a quencher<sup>7,8</sup> and (2) direct excitation in the charge-transfer (CT) band of a donor–acceptor complex (DAC).<sup>1,9</sup> However, it is generally assumed that these two pathways result in different types of ion pairs, CS quenching leading to loose or solvent-separated ion pairs (LIPs) and CT excitation to tight or contact ion pairs (TIPs).<sup>3,10</sup> Mataga and co-workers showed that these two types of ion pairs exhibit distinct free-energy-gap laws for CR.<sup>10</sup> The driving force dependence of LIPs recombination is bell-shaped, in agreement with the predictions of the semiclassical theory for nonadiabatic electron-transfer reactions.<sup>11</sup> By contrast, CR of TIPs does not become slower in the weakly exergonic region ( $\Delta G_{CR} \approx -1$  eV), but is ultrafast and takes place on the subpicosecond time scale.<sup>10,12–14</sup> It has recently been shown that this unusual free-energy-gap law for TIP recombination can be explained by a large electronic coupling that enables CR to occur before the ion pair has relaxed to equilibrium.<sup>15,16</sup> This hypothesis invoking nonequilibrium, hot recombination of TIPs has been strengthened by recent reports, where the CR of ion pairs generated by direct CT excitation was found to be nonexponential and to depend on the excitation wavelength,<sup>17</sup> as predicted by theory.<sup>18–20</sup>

We recently reinvestigated the CR dynamics of ion pairs generated upon CS quenching of perylene (Pe) in the  $S_1$  state by tetracyanoethylene (TCNE) in acetonitrile and found that, contrary to what was originally reported,<sup>21,22</sup> only a minor

fraction ( $\sim 5\%$ ) of the resulting ion pairs undergoes the slow CR expected for LIPs, whereas more than 90% of the ion pairs decay upon ultrafast recombination.<sup>23</sup> The discrepancy with the original study was due to two factors: (1) better time resolution (100 fs vs 30–50 ps) and (2) the possibility of calibrating the transient absorption signal arising from  $Pe^{*+}$  by independent photoconductivity measurements. This calibration enabled the realization that only about 10% of the ion-pair population could be observed in these measurements because the decay of most ion pairs was faster than their formation. This reinvestigation thus showed that strongly coupled ion pairs, which can be considered as TIPs, are preferentially generated even in highly exergonic bimolecular CS quenching, contrary to what is generally assumed. A qualitatively similar result was recently found for the methylperylene (MPe)/TCNE pair in acetonitrile.

The recombination dynamics of ion pairs generated by bimolecular quenching is difficult to access when both CR and CS occur on similar time scales, as the observed time evolution of the ion-pair population is a convolution of the two dynamics. In the above-mentioned studies of (MPe, Pe)/TCNE, subpicosecond CR time constants were estimated by deconvolving the independently measured CS dynamics from the experimental data.<sup>23</sup> Such a difficulty does not arise in investigations of TIPs generated by direct CT excitation. The recombination dynamics of ion pairs generated upon CT excitation of the Pe/TCNE complex was reported several years ago by Mataga and co-workers.<sup>24</sup> However, the  $\sim 500$ -fs time resolution of their experiments allowed only an approximate CR time constant of 300 fs to be estimated. Moreover, the lifetime of the ion pair was too short to permit reliable chirp-corrected absorption spectra to be resolved. Nevertheless, the observed transient band was found to be broader than that of the free  $Pe^{*+}$ .

However, to determine whether the subpicosecond time constants estimated for the recombination of ion pairs formed upon bimolecular quenching of  $MPe^*(S_1)$  and  $Pe^*(S_1)$  by TCNE are consistent with TIPs, the recombination dynamics of such TIPs generated upon CT excitation has to be established with

\* Corresponding author. E-mail: eric.vauthey@chiphys.unige.ch.

<sup>†</sup> Present address: RIKEN (The Institute of Chemical and Physical Research), 2-1 Hirosawa, Wako, Saitama 351-0198, Japan.

accuracy. Moreover, precise measurement of the absorption spectrum of the excited DAC is crucial to establish its exact nature. We present here an investigation of the CR dynamics of ion pairs generated upon CT excitation of the MPe/TCNE complex in several solvents using femtosecond visible transient absorption spectroscopy. MPe was chosen instead of Pe because of its superior solubility. However, its photophysical and electron-transfer properties are essentially the same as those of Pe.<sup>25</sup> We show that the high time resolution and signal-to-noise ratio of the measurements that can currently be readily achieved reveal a more complex excited-state dynamics than originally assumed. Ultrafast polarization sensitive measurements that yield new structural information on these complexes are also presented.

## Experimental Details

**Transient Absorption (TA) Measurements.** Excitation was performed at 800 nm using the 100-fs output pulses of a 1-kHz amplified Ti:sapphire laser system (Spectra-Physics). The energy per pulse at the sample was around 4–10  $\mu$ J. Probing was achieved with a white-light continuum obtained by focusing a small fraction of the 800-nm pulses on a H<sub>2</sub>O/D<sub>2</sub>O mixture. The probe pulses were split before reaching the sample into signal and reference pulses. The transmitted signal and reference pulses were detected with two ORIEL Multispec 125 spectrographs equipped with a 2048-pixel CCD line (Entwicklungsbüro Stresing, Berlin, Germany). Further details on the system can be found elsewhere.<sup>26</sup> All TA spectra were corrected for the chirp of the probe pulses. The polarization anisotropy,  $r(t)$ , was determined using the standard equation  $r(t) = (\Delta A_{\parallel} - \Delta A_{\perp}) / (\Delta A_{\parallel} + 2\Delta A_{\perp})$ , where  $\Delta A_{\parallel}$  and  $\Delta A_{\perp}$  are the TA signal intensities recorded with the pump-pulse polarization parallel and perpendicular, respectively, to that of the probe white-light pulses. Proper polarization of the pump and probe pulses was confirmed by an initial anisotropy value close to 0.4 ( $0.38 \pm 0.02$ ) measured with the dye IR140.

**Samples.** 3-Methylperylene (MPe) was synthesized according to the procedure reported in ref 27 and was purified twice by column chromatography on silica gel using CH<sub>2</sub>Cl<sub>2</sub> as the eluent. TCNE (Aldrich) was sublimed before use. The solvents acetonitrile (ACN), dichloromethane (DCM), and chloroform (CHCl<sub>3</sub>) were purchased from Fluka and used without further purification.

The sample solutions were contained in a 1-mm quartz cell and were continuously stirred by N<sub>2</sub> bubbling during the measurements. The concentration of the MPe/TCNE complex was adjusted to have an optical density in the range 0.2–0.4 at the excitation wavelength. The concentration of TCNE was in excess relative to that of MPe in order to avoid formation of 2:1 complexes.<sup>28</sup> No significant sample degradation was observed after the measurements. All experiments were performed at room temperature ( $23 \pm 2$  °C).

**Data Analysis.** The TA time profiles were analyzed by iterative deconvolution of the instrument response function with a sum of exponentials using a nonlinear least-square fitting procedure (MATLAB, The MathWorks, Inc., Natick, MA).

## Results

**Steady-State Absorption Spectra.** Upon addition of TCNE, originally yellowish MPe solutions become immediately dark green and exhibit a new broad absorption band around 840 nm in ACN that increases in amplitude with TCNE concentration (Figure 1). This absorption band can be assigned to a CT transition of the MPe/TCNE DAC as documented for many other complexes composed of various aromatic hydrocarbons and TCNE.<sup>29–31</sup> The rise of the CT band is accompanied by a

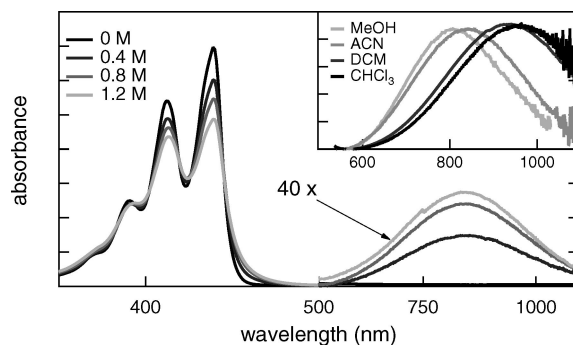


**Figure 1.** Steady-state absorption spectra of MPe with various TCNE concentrations in ACN. Inset: Intensity-normalized CT absorption band in different solvents.

**TABLE 1: Absorption Maxima of the MPe/TCNE CT Band,  $\lambda_{CT}$  and Dielectric Properties of the Solvents**

solvent	$\epsilon_s^a$	$n^b$	$\lambda_{CT}(\text{nm})$
CHCl <sub>3</sub>	4.8	1.445	965
DCM	8.9	1.424	930
MeOH	32.7	1.328	804
ACN	37.5	1.344	840

<sup>a</sup> Dielectric constant (from ref 32). <sup>b</sup> Refractive index (from ref 32).

slight decrease of the 420-nm band associated with the local S<sub>0</sub>–S<sub>1</sub> MPe transition. This effect can be interpreted as a perturbation of the electronic structure of MPe by the presence of a nearby TCNE molecule.

The inset of Figure 1 illustrates the substantial solvatochromism of the CT band (see Table 1). DACs are known to have negligibly small CT character in the ground state, so that dipole–dipole interactions should not significantly influence their CT transition energy. If this interaction were important, the CT absorption band would be red-shifted in polar solvents relative to that in nonpolar solvents, contrary to the observation. In fact, the CT transition energy decreases with increasing polarizability of the solvent molecules, which scales as  $f(n^2) = (n^2 - 1)/(n^2 + 2)$ , where  $n$  is the solvent refractive index.<sup>33</sup> A similar dependence has already been reported with other TCNE-containing DACs.<sup>33,34</sup> This indicates that the solvatochromism is most probably dominated by dispersion interactions and by dipole–dipole-induced interactions. However, the number of solvents investigated is too small to allow a more quantitative analysis.

**TA Measurements.** TA measurements upon CT excitation of MPe/TCNE at 800 nm were carried out in ACN, DCM and CHCl<sub>3</sub>. In all three solvents, a broad transient band centered at 554 nm was observed immediately after excitation. The time evolution of the TA spectrum in DCM is illustrated in Figure 2. The amplitude of the broad TA band decays substantially during the first picosecond. This decrease is accompanied by a change in the band shape, and the spectrum after 1–2 ps culminates about 10 nm below the initial one. This spectral change does not correspond to a blue shift of the TA band but rather originates from a decay of the TA intensity that is slower at the blue wing of the initial TA spectrum than at the other wavelengths. As a consequence, only this blue part of the TA spectrum survives after 1–2 ps. In DCM, the intensity of this residual TA spectrum decays to zero with an 11-ps time constant. Very similar TA spectra were obtained in ACN and CHCl<sub>3</sub>, the only difference being the temporal evolution and the relative intensity of the residual spectrum.

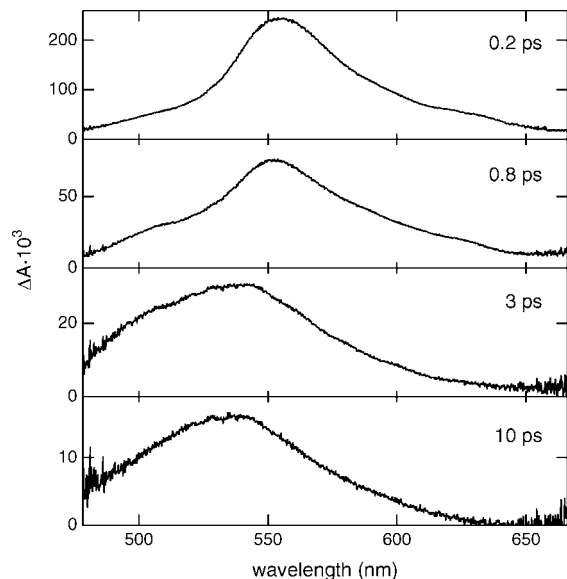


**Figure 2.** TA spectra measured at different time delays after 800-nm excitation of MPE/TCNE in DCM.

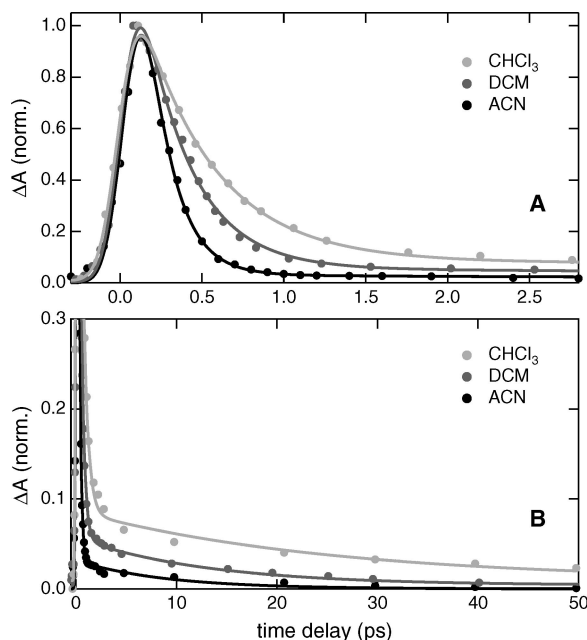


**Figure 3.** Time profiles of the TA intensity at 550 nm in the three solvents and best biexponential fit.

**TABLE 2: Best-Fit Parameters Obtained from the Analysis of the Time Profiles of TA Intensity at 550 nm<sup>a</sup>**

solvent	$\tau_1$ (fs)	$A_1$	$\tau_2$ (ps)	$A_2$
CHCl <sub>3</sub>	440	0.86	25.5	0.14
DCM	220	0.92	11.2	0.08
ACN	170	0.95	7.5	0.05

<sup>a</sup> Error limits:  $\tau_1 = \pm 5\%$ ,  $\tau_2 = \pm 15\%$ .

In the three solvents, the time profiles of the TA intensity at 550 nm (Figure 3) can be well reproduced using the convolution of the instrument response function with a biexponential function; the resulting time constants and amplitudes are listed in Table 2. Because of the small amplitude associated with the slow decay component, the error in the second time constant,  $\tau_2$ , is large. Nevertheless, it is immediately clear that both time

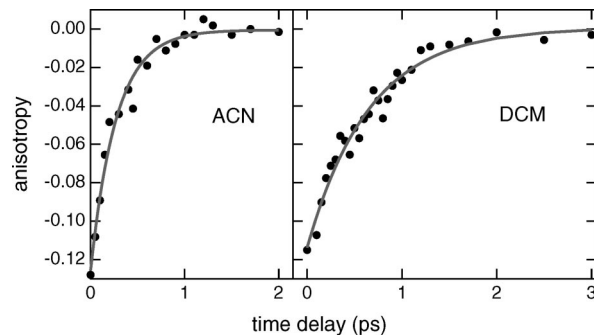


**Figure 4.** Time evolution of the polarization anisotropy at 550 nm in ACN and DCM and best single-exponential fit.

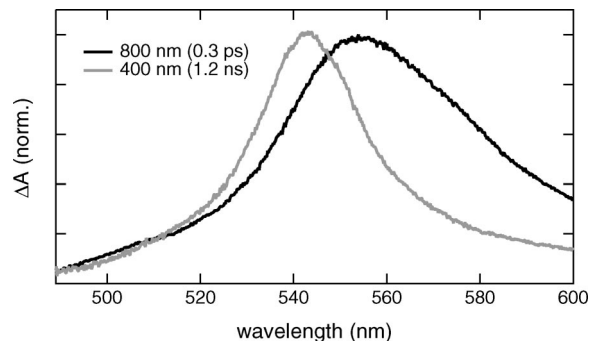


**Figure 5.** Comparison of the TA spectra recorded at early times after CT excitation at 800 nm and 1.6 ns after 400-nm excitation of MPE with 0.1 M TCNE in ACN.

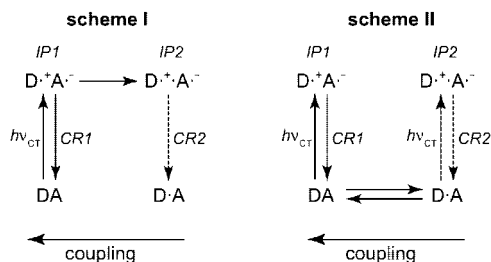
constants decrease substantially with increasing solvent polarity, as does the amplitude associated with the slow decay component,  $A_2$ .

Polarization-sensitive measurements were performed in ACN and DCM. In both solvents, the maximum TA intensity is higher with the probe beam perpendicular than with it parallel. However, this difference vanishes very quickly. As a consequence, the initial polarization anisotropy at the TA band maximum is negative,  $r_0 = -0.12 \pm 0.02$ , in both solvents. The anisotropy evolves exponentially to zero with time constants of 270 and 660 fs in ACN and DCM, respectively (Figure 4).

## Discussion

The TA spectra recorded upon 800-nm excitation of the MPE/TCNE complex can undoubtedly be ascribed to a species with a strong CT character. However, the early TA spectrum culminating at 554 nm differs to some extent from that of MPE<sup>•+</sup> generated by bimolecular quenching of MPE\*(S<sub>1</sub>) by TCNE. Figure 5 shows a comparison of the TA spectrum recorded 1.2 ns after local excitation of MPE at 400 nm with 0.1 M TCNE with that measured directly after 800-nm excitation of the complex. The former spectrum is very similar to the well-documented spectrum of Pe<sup>•+</sup>, with an intense band related to the D<sub>0</sub> → D<sub>5</sub> transition peaking at 543 nm and a width of about 1000 cm<sup>-1</sup>,<sup>21,35,36</sup> whereas the width of latter spectrum is 1650 cm<sup>-1</sup>. This greater width and red-shifted maximum can be assigned to an incomplete CT character of the excited DAC. The wavefunction associated with such a state is usually discussed in terms of a linear combination of the wavefunctions of the neutral ground state; of the pure CT state, D<sup>•+</sup>A<sup>•-</sup>; and of the locally excited states, D<sup>\*</sup>A and DA<sup>\*</sup>.<sup>37,38</sup> For the present pair, the DA<sup>\*</sup> state is at much higher energy than the D<sup>\*</sup>A state, and its contribution to the excited DAC wavefunction can be neglected. As the absorption spectrum of MPE\*(S<sub>1</sub>) consists in

CHART 1



an intense band centered at 700 nm, some admixture of the D<sup>•+</sup>A<sup>•-</sup> wavefunction with that of D<sup>•+</sup>A<sup>•-</sup> could lead to the observed broad and red-shifted TA spectrum. This interpretation is corroborated by recent TA measurements performed with nitroperylene (NPe).<sup>39</sup> In nonpolar solvents, the TA spectrum of NPe upon S<sub>0</sub>–S<sub>1</sub> excitation is very similar to that of the parent Pe, indicating an essentially zero CT character of the excited state. In polar solvents, on the other hand, the TA spectrum is broader and peaks between those of Pe<sup>•+</sup> and Pe<sup>•</sup>, pointing to a substantial CT character of the excited state. This partial CT character is further supported by the fluorescence spectrum of NPe, which is essentially identical to that of Pe in nonpolar solvents but is structureless and red-shifted in polar solvents, indicative of CT-type fluorescence.

No CT emission could be observed with the MPe/TCNE complex. However, such fluorescence should be very difficult to detect because it should be located in the near-infrared and because its quantum yield should be negligibly small, considering the lifetime of the CT state.

Both spectral broadening and red shifting are also characteristic of a vibrationally hot electronic state.<sup>40</sup> However, this should not be a significant factor for the spectral differences shown in Figure 5, as the amount of excess excitation energy at 800 nm is not large, around 0.3–0.4 eV. Moreover, the early TA spectrum recorded upon 400-nm excitation of MPe with 0.9 M TCNE is essentially as narrow as that depicted in Figure 5, despite the formation of ion pairs with about 2 eV excess energy.<sup>23</sup>

The TA band recorded several picoseconds after CT excitation (Figure 2) is also considerably broader than that of MPe<sup>•+</sup> but peaks at the same wavelength. The greater width of this residual band might partially be due to the weakness of the signal. The coincidence of its maximum with that of MPe<sup>•+</sup> is indicative of a state with greater CT character than that associated with the early red-shifted spectrum.

Two reaction schemes can be envisaged to explain the TA results (see Chart 1). In the serial model (scheme I), an excited DAC that can be viewed either as a very strongly coupled ion pair (IP1) or as an excited state with an incomplete CT character is first generated. The population of this state either decays by CR to the ground state or evolves to another state characterized by greater CT character that can be considered as a less coupled ion pair (IP2). Finally, this IP2 population recombines to the neutral ground state.

The parallel model in scheme II is based on the assumption that the ground-state complex can exist in different geometries, with various values of the electronic coupling,  $V$ , and thus different oscillator strengths for CT absorption,  $f_{CT}$ , as  $f_{CT} \propto V^2$ . Light at 800 nm thus predominantly excites strongly coupled DACs and also interacts, but to a much lesser extent, with more weakly coupled complexes. Because the CR dynamics in the ensuing ion pairs depends on the overlap of the same molecular orbitals than CT excitation, hence on  $V^2$ , DACs with the highest

probability to be excited are also those that undergo faster recombination. According to this scheme, the early TA spectrum is therefore due to both types of excited DACs, IP1 + IP2, whereas the late spectrum originates from IP2 only.

The CT character of IP1 is not full because of the strong overlap of the molecular orbitals of the constituents, whereas complete CT is possible only with a vanishingly small overlap. As a consequence, the IP1 absorption spectrum is red-shifted as the excited DAC wavefunction contains some admixture of the D<sup>•+</sup>A<sup>•-</sup> state. For the same reason, IP2 has greater CT character, and its absorption spectrum more closely resembles that of the individual ions.

Discriminating between schemes I and II from the TA data is difficult, as the IP2 population is very small compared to that of IP1. According to scheme I, the transition from IP1 to IP2 should lead to an increase of the TA signal at short wavelength. However, the absence of such an increase does not completely undermine scheme I because of the relatively small IP2 population. From scheme I, the quantum yield of IP2 formation is

$$\Phi_{IP2} = \frac{k_{12}}{k_{12} + k_{CR1}} = k_{12}\tau_1 \quad (1)$$

where  $k_{12}$  is the rate constant of the IP1-to-IP2 transition,  $k_{CR1}$  is the rate constant of IP1 recombination, and  $\tau_1$  is the time constant related to the fast decay component of the TA signal. As the relative amplitude of the slow decay component,  $A_2$ , gives a good estimate of  $\Phi_{IP2}$ ,  $k_{12}$  can be directly calculated with eq 1. The resulting  $k_{12}$  values are rather close to each other and amount to (3.4 ps)<sup>-1</sup>, (2.75 ps)<sup>-1</sup>, and (3.14 ps)<sup>-1</sup> in ACN, DCM, and CHCl<sub>3</sub>, respectively. In principle, the IP1-to-IP2 transition can be expected to involve some intracomplex and/or solvent reorganization. Intracomplex rearrangement should presuppose some changes in the mutual orientation of the constituents and should thus depend on solvent viscosity. Such a dependence is obviously not present here, the smallest  $k_{12}$  being found in the least viscous solvent, ACN. A correlation between the calculated  $k_{12}$  values and the solvation time constants reported in the literature<sup>41</sup> is absent as well. For example, solvation in ACN is, on average, 10 times faster than that in CHCl<sub>3</sub>.<sup>41</sup> Therefore, scheme I is not supported by the experimental data, as it is difficult to justify such  $k_{12}$  values. It should be noted that some spectral narrowing of the TA band due to the relaxation of the excited DACs from the Franck–Condon state toward equilibrium has already been reported.<sup>16,24,42</sup> In those cases, however, the decay of the TA band integral was essentially monophasic, contrary to the results obtained here, and the time scale of the spectral dynamics depended on the solvent viscosity and polarity.<sup>16,24</sup>

Scheme II, on the other hand, implies different MPe/TCNE complexes. There is much evidence that several DA pairs can form complexes with different mutual orientations of the constituents. For example, complexes with substituted benzenes, such as anisole, and TCNE and exhibit two CT absorption bands, where the low- and high-energy bands correspond to a single-electron transition from the HOMO and HOMO – 1, respectively, of D to the LUMO of A.<sup>29–31</sup> As the HOMO and HOMO – 1 of D do not have the same symmetry, a substantial overlap with the LUMO of A implies different mutual orientations of D and A and, thus, different DAC geometries.<sup>43,44</sup> It has been recently shown that the CR dynamics of DACs exhibiting two CT bands depends on which of the two CT transitions is excited.<sup>17</sup>

Braun and co-workers reported that the free ion yield measured with DACs composed of alkylbenzenes and TCNE in DCM varies continuously with the CT excitation wavelength.<sup>45</sup> It was found to be the smallest upon excitation at the center of the CT band and to increase by a factor of up to 100 for excitation on the band edges. This result was explained in terms of “random DA pairs” that have a relatively large center-to-center distance and thus a high probability to dissociate into free ions when excited. Because of this greater distance, these random pairs have a much smaller absorption coefficient and a blue-shifted spectrum.<sup>46</sup>

Scheme II agrees qualitatively very well with the model of Braun and co-workers, with the random pairs corresponding to the more weakly coupled IP2. This hypothesis is further supported by two experimental observations: (1) the fast decay of the polarization anisotropy and (2) the solvent dependence of  $A_2$ .

First, the polarization anisotropy decays substantially faster than the TA signal intensity, with a time constant close to  $\tau_1$ . This indicates that this anisotropy is almost entirely associated with the strongly coupled IP1. Considering that the TA intensity arises from two populations, IP1 + IP2, the time dependence of the anisotropy, assuming no loss through reorientational motion, is given by

$$r(t) = \frac{\sum_{i=1}^2 c_i(t)r_{0i}}{\sum_{i=1}^2 c_i(t)} \quad (2)$$

where  $c_i(t) = A_i \exp(-\tau_i t)$ , with  $A_i$  and  $\tau_i$  being the amplitudes and time constants, respectively, found from the analysis of the TA time profiles at 550 nm (Table 1), and  $r_{0i}$  is the initial anisotropy related to IP $_i$ . If  $r_{01} = r_{02}$ , the anisotropy remains constant as long as reorientational motion does not occur. For molecules of the size as MPE and TCNE, reorientation in ACN can be expected to take place with a time constant of the order of 10 ps or more,<sup>25</sup> i.e. much greater than the anisotropy decay time found here.

The fact that the measured polarization anisotropy vanishes completely within 2–3 ps points to a zero or close-to-zero value of  $r_{02}$ , the initial anisotropy associated with IP2. In this case, the initial anisotropy found experimentally,  $r_0$ , corresponds to

$$r_0 = A_1 r_{01} \quad (3)$$

Thus, according to this equation,  $r_{01}$ , the initial polarization anisotropy associated with IP1, amounts to about  $-0.13$  in both ACN and DCM.

A nonzero anisotropy at 550 nm indicates that the orientations of the CT transition dipole moment of the complex and the  $D_0$ – $D_5$  transition dipole moment of  $MPE^{++}$  are correlated. This implies a relatively well-defined mutual orientation of the constituents. The angle  $\gamma$  between the two transition dipole moments can be calculated from the expression<sup>47</sup>

$$r_0 = (3 \cos^2 \gamma - 1)/5 \quad (4)$$

With  $r_{10} = -0.13$ , this equation yields  $\gamma = 70^\circ$ , a value rather similar to that already reported for other DACs.<sup>48</sup> This value has a physical meaning only if all IP1-type pairs have the same geometry. If this were not the case, then the  $r_{10}$  value would correspond to an average over all the initial anisotropies associated with each geometry. Assuming a coplanar geometry of the complex with the CT transition dipole moment pointing

from the center of MPE to the center of TCNE and knowing that the  $D_0$ – $D_5$  transition dipole moment of  $MPE^{++}$  lies along the long molecular axis,<sup>49</sup> a  $70^\circ$  angle is realized in a geometry in which TCNE faces one of the two naphthalenic parts of MPE. This is a physically reasonable geometry as it gives greater coupling than the geometry in which MPE and TCNE are face-centered. The latter structure would result in an initial anisotropy of  $-0.2$ , clearly beyond the limit of error in  $r_0$ .

Considering the time scale of the experiment, the anisotropy provides information on the Franck–Condon excited-state geometry, which thus reflects the ground-state equilibrium geometry of the DAC. Given the substantial change of electronic distribution upon CT excitation, the equilibrium geometry of the excited DAC can be expected to differ substantially. However, the lifetime of IP1 is too short for such equilibrium to be attained.

As the polarization anisotropy related to the longer-lived IP2 is essentially zero, one can conclude that, unlike IP1, this ion pair has a much less precise geometry, in agreement with the random-pair picture.<sup>46</sup> However, the absence of polarization anisotropy could also stem from a complex with well-defined mutual orientation of the constituents but a  $\gamma$  value close to  $54.7^\circ$ .

Although much less structural information on IP2 can be inferred from the data, the coupling in these ion pairs must still be large enough to afford a sufficient absorption coefficient and a CR occurring within a few picoseconds. As a consequence, the D and A constituents are still probably at contact distance but with a mutual orientation that does not lead to optimal coupling.

The second observation in favor of scheme II concerns the solvent dependence of  $A_2$ , the amplitude of the slow decay component. As shown in Table 2,  $A_2$  increases from ACN to DCM and  $CHCl_3$ , indicating a larger relative population of IP2. Moreover, the difference between the absorption band maximum and the excitation wavelength also increases from ACN to DCM and  $CHCl_3$  (Table 1). Indeed, 800 nm is close to the CT absorption maximum in ACN where  $A_2$  is the smallest, whereas in DCM and especially in  $CHCl_3$  where  $A_2$  is the largest, this wavelength coincides with the blue wing of the CT band. Theoretical analysis by Braun, Sutin, and co-workers showed that the CT absorption spectrum of random pairs is blue-shifted relative to that of the “normal” DACs.<sup>46</sup> This is completely consistent with our observations:  $A_2$  is the largest in  $CHCl_3$  because, in this solvent, excitation is performed on the far blue side of the absorption band, where random pairs have the highest probability of absorbing. In ACN, on the other hand, excitation is near the maximum of the CT band, where random pairs have a low probability to interact.

All of these observations strongly support scheme II over scheme I.

The fast decay component found here with the MPE/TCNE system is among the fastest measured for a CR process. In all three solvents,  $\tau_1$  is substantially shorter than the corresponding time constant for diffusive solvent motion, which ranges from about 600 fs for ACN to more than 4 ps for  $CHCl_3$ .<sup>41</sup> Such CR faster than diffusive solvation has already been reported for several DACs<sup>16,17</sup> and has been explained in terms of hot or nonequilibrium CR using an hybrid model proposed by Barbara and coworkers<sup>50,51</sup> that combines the two-dimensional Sumi–Marcus<sup>52</sup> and nonadiabatic semiclassical electron-transfer theories.<sup>53</sup> On the other hand,  $\tau_2$  is larger than the diffusive solvation time constants, pointing to CR from equilibrated ion pairs. The regime in which CR takes place, namely, equilibrium

or nonequilibrium, depends only on the magnitude of the electronic coupling.

Finally, it should be noted that  $\tau_2$  most probably corresponds not to a single time constant but to an average value reflecting a distribution of mutual DA orientations in IP2. Such a distribution could also account for the relatively large width of the residual TA band (Figure 2).

The CR time constants measured here for ion pairs produced upon direct CT excitation agree well with those found for ion pairs generated upon bimolecular CS in ACN.<sup>23,54</sup> In the latter case, the subpicosecond CR component could be deduced only through a rather complex deconvolution of CS and CR dynamics from the observed TA signal. A 5–10-ps CR time constant was also found at high TCNE concentration.<sup>23</sup> The main difference between CT excitation and bimolecular CS is the presence, in the latter case, of an even slower CR component with a 100–200-ps time constant and the formation of free ions. This is clear evidence that the distribution of ion-pair geometries is much wider upon bimolecular CS. This results in a large span of CR time constants going from a few hundreds of femtoseconds to values similar to or greater than the time constant for dissociation into free ions, which is on the order of 1 ns in ACN.<sup>55–58</sup>

### Concluding Remarks

The present investigation sheds new light on the excited-state dynamics of DACs. Contrary to what is generally assumed, direct CT excitation results in the formation of several types of ion pairs differing by their coupling. In the present case, these ion pairs could be differentiated by their distinct absorption spectra, polarization anisotropy, and recombination dynamics. The ion pairs formed upon direct CT excitation of DACs do not fundamentally differ from those generated upon bimolecular CS quenching, as the main difference is a narrower distribution of the mutual orientations of the ions. The distribution of electronic coupling constants is also substantially narrower and does not extend to very low values. Therefore, CT excitation leads, in most cases, to much smaller free ion yield than bimolecular quenching.

Although DACs have been intensively investigated over the past several decades, their structure in solution and the donor–acceptor pair distribution in the ground state are still essentially unknown. The latter plays a fundamental role in the nature of the ion pairs generated by both CT excitation and bimolecular quenching.<sup>59–61</sup> Considerable theoretical and experimental work is still needed before a comprehensive picture is obtained.

**Acknowledgment.** The authors thank Prof. Anatoly I. Ivanov (Volgograd State University) for his fruitful comments. This work was supported by the Fonds National Suisse de la Recherche Scientifique through Project 200020-115942.

### References and Notes

- Masnovi, J. M.; Kochi, J. K. *J. Am. Chem. Soc.* **1985**, *107*, 7880.
- Peters, K. S.; Lee, J. *J. Am. Chem. Soc.* **1993**, *115*, 3643.
- Gould, I. R.; Farid, S. *Acc. Chem. Res.* **1996**, *29*, 522.
- Mataga, N.; Miyasaka, H. *Adv. Chem. Phys.* **1999**, *107*, 431.
- Vauthey, E. *J. Photochem. Photobiol. A* **2006**, *179*, 1.
- Kuzmin, M. G.; Soboleva, I. V.; Dolotova, E. V. *J. Phys. Chem. A* **2007**, *111*, 206.
- Leonhardt, H.; Weller, A. *Z. Phys. Chem. N. F.* **1961**, *277*.
- Weller, A. *Pure Appl. Chem.* **1982**, *54*, 1885.
- Gould, I. R.; Moody, R.; Farid, S. *J. Am. Chem. Soc.* **1988**, *110*, 7242.

- Asahi, T.; Mataga, N. *J. Phys. Chem.* **1989**, *93*, 6575.
- Marcus, R. A.; Sutin, N. *Biochim. Biophys. Acta* **1985**, *811*, 265.
- Hubig, S. M.; Bockman, T. M.; Kochi, J. K. *J. Am. Chem. Soc.* **1996**, *118*, 3842.
- Wynne, K.; Galli, C.; Hochstrasser, R. M. *J. Chem. Phys.* **1994**, *100*, 4797.
- Jarzeba, W.; Pommeret, S.; Mialocq, J.-C. *Chem. Phys. Lett.* **2001**, *333*, 419.
- Tachiya, M.; Murata, S. *J. Am. Chem. Soc.* **1994**, *116*, 2434.
- Nicolet, O.; Vauthey, E. *J. Phys. Chem. A* **2002**, *106*, 5553.
- Nicolet, O.; Banerji, N.; Pagès, S.; Vauthey, E. *J. Phys. Chem. A* **2005**, *109*, 8236.
- Ivanov, A. I.; Belikeev, F. N.; Fedunov, R. G.; Vauthey, E. *Chem. Phys. Lett.* **2003**, *372*, 73.
- Fedunov, R. G.; Feskov, S. V.; Ivanov, A. I.; Nicolet, O.; Pagès, S.; Vauthey, E. *J. Chem. Phys.* **2004**, *121*, 3643.
- Feskov, S. V.; Ionkin, V. N.; Ivanov, A. I.; Hagemann, H.; Vauthey, E. *J. Phys. Chem. A* **2008**, *112*.
- Mataga, N.; Kanda, Y.; Okada, T. *J. Phys. Chem.* **1986**, *90*, 3880.
- Mataga, N.; Kanda, Y.; Asahi, T.; Miyasaka, H.; Okada, T.; Kakitani, T. *Chem. Phys.* **1988**, *127*, 239.
- Pagès, S.; Lang, B.; Vauthey, E. *J. Phys. Chem. A* **2004**, *108*, 549.
- Asahi, T.; Mataga, N. *J. Phys. Chem.* **1991**, *95*, 1956.
- Morandira, A.; Fürstenberg, A.; Gumy, J.-C.; Vauthey, E. *J. Phys. Chem. A* **2003**, *107*, 5375.
- Duvanel, G.; Banerji, N.; Vauthey, E. *J. Phys. Chem. A* **2007**, *111*, 5361.
- Buu-Hoï, N. P.; Long, C. T. *Rec. Trav. Chim. Pays-Bas* **1956**, *75*, 1221.
- Smith, M. L.; McHale, J. L. *J. Phys. Chem.* **1985**, *89*, 4002.
- Orgel, L. E. *J. Chem. Phys.* **1955**, *23*, 1352.
- Voigt, E.-M. *J. Am. Chem. Soc.* **1964**, *86*, 3611.
- Rossi, M.; Buser, U.; Haselbach, E. *Helv. Chim. Acta* **1976**, *59*, 1039.
- Riddick, J. A.; Bunger, W. B. *Organic Solvents*; Wiley: New York, 1970.
- Suppan, P.; Ghoneim, N. *Solvatochromism*; The Royal Society of Chemistry: Cambridge, U.K., 1997.
- Rosenberg, H. M.; Hale, D. *J. Phys. Chem.* **1965**, *69*, 2490.
- Shida, T. *Electronic Absorption Spectra of Radical Ions*; Physical Sciences Data Series; Elsevier: Amsterdam, 1988; Vol. 34.
- Gumy, J.-C.; Vauthey, E. *J. Phys. Chem. A* **1997**, *101*, 8575.
- Murrell, J. N. *J. Am. Chem. Soc.* **1959**, *81*, 5037.
- Bender, C. *J. Chem. Soc. Rev.* **1986**, *15*, 475.
- Mohammed, O. F.; Vauthey, E. *J. Phys. Chem. A* **2008**, *112*, 3823.
- Gottfried, N. H.; Seilmeier, A.; Kaiser, W. *Chem. Phys. Lett.* **1984**, *111*, 326.
- Horng, M. L.; Gardecki, J. A.; Papazyan, A.; Maroncelli, M. *J. Phys. Chem.* **1995**, *99*, 17311.
- Ojima, S.; Miyasaka, H.; Mataga, N. *J. Phys. Chem.* **1990**, *94*, 5834.
- Mobley, M. J.; Rieckhoff, K. E.; Voigt, E.-M. *J. Phys. Chem.* **1977**, *81*, 809.
- Michaelian, K. H.; Rieckhoff, K. E.; Voigt, E.-M. *Proc. Natl. Acad. Sci. U.S.A.* **1975**, *72*, 4196.
- Zhou, J.; Findley, B. R.; Teslja, A.; Braun, C. L.; Sutin, N. *J. Phys. Chem. A* **2000**, *104*, 11512.
- Zhou, J.; Findley, B. R.; Braun, C. L.; Sutin, N. *J. Chem. Phys.* **2001**, *114*, 10448.
- Weber, G. *J. Chem. Phys.* **1971**, *55*, 2399.
- Arnold, B. R.; Schill, A. W.; Poliakov, P. V. *J. Phys. Chem. A* **2001**, *105*, 537.
- Hiratsuka, H.; Hatano, Y.; Tanizaki, Y.; Mori, Y. *J. Chem. Soc., Faraday Trans. 2* **1985**, *81*, 1653.
- Walker, G. C.; Akesson, E.; Johnson, A. E.; Levinger, N. E.; Barbara, P. F. *J. Phys. Chem.* **1992**, *96*, 3728.
- Barbara, P. F.; Walker, G. C.; Smith, T. P. *Science* **1992**, *256*, 975.
- Sumi, H.; Marcus, R. A. *J. Chem. Phys.* **1986**, *84*, 4894.
- Kestner, N. R.; Logan, J.; Jortner, J. *J. Phys. Chem.* **1974**, *78*, 2148.
- Vauthey, E. *J. Phys. Chem. A* **2001**, *105*, 340.
- Mataga, N.; Asahi, T.; Kanda, Y.; Okada, T.; Kakitani, T. *Chem. Phys.* **1988**, *127*, 249.
- Vauthey, E. *J. Phys. Chem. A* **2000**, *104*, 1804.
- Pagès, S.; Lang, B.; Vauthey, E. *J. Phys. Chem. A* **2006**, *110*, 7547.
- Mohammed, O. F.; Banerji, N.; Lang, B.; Nibbering, E. T. J.; Vauthey, E. *J. Phys. Chem. A* **2006**, *110*, 13676.
- Burshtein, A. I. *Adv. Chem. Phys.* **2000**, *114*, 419.
- Burshtein, A. I. *Adv. Chem. Phys.* **2004**, *129*, 105.
- Gladkikh, V.; Burshtein, A. I.; Angulo, G.; Pagès, S.; Lang, B.; Vauthey, E. *J. Phys. Chem. A* **2004**, *108*, 6667.